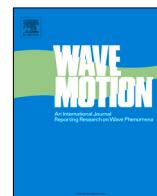# Scattering of elastic waves by a transversely isotropic sphere and ultrasonic attenuation in hexagonal polycrystalline materials

(article starts on next page)

Scattering of elastic waves by a transversely isotropic sphere and ultrasonic attenuation in hexagonal polycrystalline materials

Ata Jafarzadeh *, Peter D. Folkow, Anders Boström

Chalmers University of Technology, Department of Mechanics and Maritime Sciences, Horsalsvagen 7, SE-412 96 Gothenburg, Sweden

ABSTRACT

The scattering of elastic waves by a transversely isotropic sphere in an isotropic medium is considered. The elastodynamic equations inside the sphere are transformed to spherical coordinates and the displacement field is expanded in the vector spherical harmonics in the angular coordinates and powers in the radial coordinate. The governing equations inside the sphere then give recurrence relations among the expansion coefficients. Then all the remaining expansion coefficients for the fields outside and inside the sphere are found using the boundary conditions on the surface of the sphere. As a result, the transition (**T**) matrix elements are calculated and given explicitly for low frequencies. Using the **T** matrix and the theory of Foldy an explicit expression for the effective complex wave number of transversely isotropic (hexagonal) polycrystalline materials are presented for low frequencies. Numerical comparisons are made with previously published results and with recent FEM results and show a very good correspondence with FEM for low frequencies. As opposed to other published methods there is no limitation on the degree of anisotropy with the present approach.

© 2022 The Authors. Published by Elsevier B.V. This is an open access article under the CC BY license (http://creativecommons.org/licenses/by/4.0/).

1. Introduction

Scattering of waves by a single obstacle is a classical problem in mathematical physics. The wave scattered by an obstacle can be calculated in various well-known ways, such as by the method of separation-of-variables, the **T** matrix methods, integral equation methods, and finite element (FE) methods. A comprehensive overview of scattering of acoustic, electromagnetic, and elastic waves in isotropic media is presented in a unified way by de Hoop [1] and Varadan et al. [2]. Wave propagation through an elastic medium with a distribution of inclusions is also studied by many authors, the objective often being to characterize such media by ultrasonic means. A simple approach to deal with such problems is presented by Foldy [3]. The theory of Foldy neglects multiple scattering and estimates the effective wave numbers of the medium by the scattering cross section of a single inclusion and the number density of inclusions. This is used by many authors to study wave propagation through an isotropic elastic medium with a distribution of isotropic inclusions, see for instance [4,5].

However, there exist many anisotropic materials, which may be natural or synthetic. For instance, natural soils and rocks, fiber composites, or the grains in a metal are all anisotropic. Studying wave propagation in anisotropic materials is more complicated since many of the classical methods are not applicable any longer. Wave propagation in anisotropic

* Corresponding author.
  E-mail address: jata@chalmers.se (A. Jafarzadeh).

materials has, therefore, mostly been studied for unbounded and semi-bounded media. For finite obstacles, where the interest of the current study lies, not much has been done and then mostly for electromagnetic waves (see, [6–8]). For mechanical waves, spherically and cylindrically anisotropic obstacles are considered by some authors [9–13]. 2D scattering of elastic waves by an anisotropic (in Cartesian coordinates) obstacle is investigated by Boström using expansions in trigonometric functions in the angular coordinate and powers in the radial coordinate [14,15]. Recently the same method is used for scattering of SH (torsional) waves by a transversely isotropic sphere in the special axisymmetric case and the **T** matrix elements are presented explicitly [16].

A special case of anisotropy appears in polycrystalline materials (typically metals), where the grains are anisotropic. If the grains are equiaxed and randomly oriented the overall properties of the material still becomes isotropic. To estimate attenuation and effective wave speed in polycrystals various approximate methods are used. Most of these estimations are using volume integral equation methods combined with some perturbation method, often the Born approximation. For instance, Stanke and Kino [17] calculate the wave speed and attenuation using this method, Thompson et al. [18] give an overview of scattering of elastic waves in simple and complex polycrystals, Yang et al. [19] present an explicit model for ultrasonic attenuation in equiaxed hexagonal polycrystalline materials, and Li and Rokhlin [20] study the scattering in general random anisotropic solids. All these methods are valid more or less for all frequencies, however, they seem to have restrictions to relatively weak anisotropy. Recently finite element methods (FEM) have also been used to study polycrystalline materials and investigate the attenuation and phase velocity in them, see [21–26] (these papers contain very readable introductions to the field and many further references).

A different type of approach is obtained if the scattering by each grain in the polycrystal material is regarded as taking place in the effective, homogeneous and isotropic medium of all other grains (assuming that the grains are equiaxed and randomly oriented) thus the wave propagation in polycrystalline materials can be viewed as a special case of a distribution of inclusions. Boström and Ruda [27] use this approach to estimate the attenuation of 2D polycrystalline materials with grains of cubic material. Starting from the explicit transition matrix for cubic materials presented by Boström [15] the scattering cross section is obtained and then the attenuation is estimated using an energy consideration. Such an approach does not have any limitation on the degree of anisotropy, however, it is restricted to low frequencies.

In this article the scattering of an elastic wave is considered for a single transversely isotropic (in Cartesian coordinates) spherical obstacle contained in an isotropic elastic medium. The starting point is to state the anisotropic elastodynamic equations in spherical coordinates. The equations then contain trigonometric functions only in the polar coordinate, while for materials with lack of rotational symmetry (e.g. cubic symmetry) there are trigonometric functions in the azimuthal coordinate as well, which lead to more complex elastodynamic equations. Expanding the displacement field in terms of the vector spherical harmonics for the angular dependence and power series for the radial dependence, the elastodynamic equations give recursion relations among the expansion coefficients. Using the boundary conditions on the surface of the sphere results in a system of equations for all the remaining expansion coefficients of the fields outside and inside the sphere. Solving the system of equation provides the **T** matrix for the scattering by a single sphere. The leading order **T** matrix elements are derived explicitly for low frequencies. The attenuation and phase velocity of polycrystalline materials containing transversely isotropic grains is estimated for low frequencies using the theory of Foldy and the **T** matrix, see [4,5]. It is particularly noted that the weak anisotropy assumption, which seems to be made for most other analytical methods, is not made in the present approach.

2. Statement of the problem

The scattering of an elastic wave by a transversely isotropic sphere with radius a in a three-dimensional, homogeneous, infinite elastic medium is considered (Fig. 1). The material of the surrounding infinite medium is assumed isotropic with density ρ and Lamé parameters λ and μ. The description of the sphere and its material properties is left for Section 3. Only time harmonic situations are considered and the time factor $\exp(-i\omega t)$, where ω is the angular frequency and t is time, is suppressed throughout. Introducing the longitudinal and transverse wave numbers $k_p^2 = \rho\omega^2/(\lambda + 2\mu)$ and $k_s^2 = \rho\omega^2/\mu$, respectively, the equation of motion in terms of the displacement field $\boldsymbol{u}$ is

$$\frac{1}{k_p^2}\nabla(\nabla \cdot \boldsymbol{u}) - \frac{1}{k_s^2}\nabla \times (\nabla \times \boldsymbol{u}) + \boldsymbol{u} = 0. \tag{1}$$

For a spherical obstacle it is natural to use spherical coordinates (r, θ, φ) to describe the field quantities. For expressing the displacement field in the surrounding medium, it is convenient to introduce the spherical vector wavefunctions $\boldsymbol{\psi}_{\tau\sigma ml}$. Solving the governing differential equations in the isotropic medium (Eq. (1)) the following three spherical vector wavefunctions are defined

$$\boldsymbol{\psi}_{1\sigma ml}^0(r, \theta, \varphi) = \frac{1}{\sqrt{l(l+1)}}\nabla \times \left(j_l(k_s r)Y_{\sigma ml}(\theta, \varphi)\right) = j_l(k_s r)\boldsymbol{A}_{1\sigma ml}(\theta, \varphi), \tag{2}$$

$$\begin{aligned}\boldsymbol{\psi}_{2\sigma ml}^0(r, \theta, \varphi) &= \frac{1}{\sqrt{l(l+1)}}\nabla \times \nabla \times \left(j_l(k_s r)Y_{\sigma ml}(\theta, \varphi)\right) \\ &= \left(j_l'(k_s r) + \frac{j_l(k_s r)}{k_s r}\right)\boldsymbol{A}_{2\sigma ml}(\theta, \varphi) + \sqrt{l(l+1)}\frac{j_l(k_s r)}{k_s r}\boldsymbol{A}_{3\sigma ml}(\theta, \varphi),\end{aligned} \tag{3}$$
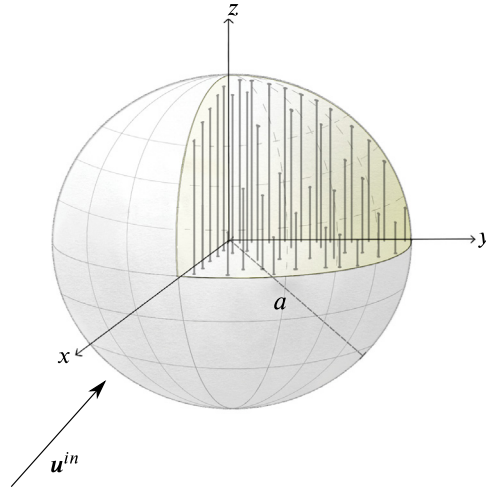
Fig. 1. The transversely isotropic sphere with radius a and the incident wave.

$$
\begin{aligned}
\boldsymbol{\psi}^0_{3\sigma ml}(r, \theta, \varphi) &= \left(\frac{k_p}{k_s}\right)^{3/2} \frac{1}{k_p} \nabla \left(j_l(k_p r) Y_{\sigma ml}(\theta, \varphi) \right) \\
&= \left(\frac{k_p}{k_s}\right)^{3/2} \left(j'_l(k_p r) \boldsymbol{A}_{3\sigma ml}(\theta, \varphi) + \sqrt{l(l+1)} \frac{j_l(k_p r)}{k_p r} \boldsymbol{A}_{2\sigma ml}(\theta, \varphi) \right),
\end{aligned}
\tag{4}
$$

where the indices run through $l = 0, 1, 2, \ldots$, $m = 0, 1, \ldots, l$, $\sigma = e$ (even), o (odd), and the first index is denoted $\tau = 1, 2, 3$ for SH, SV and P wavefunctions, respectively. For $l = 0$ only the $\tau = 3$ wavefunction is relevant; for $l = 0$ the wavefunctions for $\tau = 1, 2$ are not defined. The upper index 0 specifies the regular wavefunctions which contain spherical Bessel functions j_l. The corresponding outgoing wavefunctions are denoted with the upper index $+$ and contain spherical Hankel functions $h_l^{(1)}$ to satisfy the radiation condition in the far field. $\mathbf{A}_{\tau\sigma ml}$ are the vector spherical harmonics defined as

$$
\begin{aligned}
\boldsymbol{A}_{1\sigma ml}(\theta, \varphi) &= \frac{1}{\sqrt{l(l+1)}} \nabla \times (\boldsymbol{r} Y_{\sigma ml}(\theta, \varphi)) = \frac{1}{\sqrt{l(l+1)}} \left(\boldsymbol{e}_\theta \frac{1}{\sin\theta} \frac{\partial}{\partial\varphi} Y_{\sigma ml}(\theta, \varphi) - \boldsymbol{e}_\varphi \frac{\partial}{\partial\theta} Y_{\sigma ml}(\theta, \varphi) \right), \\
\boldsymbol{A}_{2\sigma ml}(\theta, \varphi) &= \frac{1}{\sqrt{l(l+1)}} r \nabla Y_{\sigma ml}(\theta, \varphi) = \frac{1}{\sqrt{l(l+1)}} \left(\boldsymbol{e}_\theta \frac{\partial}{\partial\theta} Y_{\sigma ml}(\theta, \varphi) + \boldsymbol{e}_\varphi \frac{1}{\sin\theta} \frac{\partial}{\partial\varphi} Y_{\sigma ml}(\theta, \varphi) \right), \\
\boldsymbol{A}_{3\sigma ml}(\theta, \varphi) &= \boldsymbol{e}_r Y_{\sigma ml}(\theta, \varphi).
\end{aligned}
\tag{5}
$$

Here $Y_{\sigma ml}$ is a spherical harmonic with the following definition

$$
Y_{\sigma ml}(\theta, \varphi) = \sqrt{\frac{\epsilon_m (2l+1)(l-m)!}{4\pi(l+m)!}} P_l^m(\cos\theta) \left\{ \begin{array}{c} \cos m\varphi \\ \sin m\varphi \end{array} \right\},
\tag{6}
$$

where $P_l^m(\cos\theta)$ is an associated Legendre function and where $\sigma = e$ is for the upper row which is even with respect to φ and $\sigma = o$ is for the lower row which is odd with respect to φ.

The surface tractions on $r = a$ are necessary to apply the boundary conditions. The radial traction field in the isotropic medium, which of course has the components $\sigma_{rr}, \sigma_{r\theta}$ and $\sigma_{r\varphi}$, is given by

$$
\boldsymbol{t}^{(r)} = \boldsymbol{e}_r \lambda \nabla \cdot \boldsymbol{u} + \mu \left(2 \frac{\partial \boldsymbol{u}}{\partial r} + \boldsymbol{e}_r \times (\nabla \times \boldsymbol{u}) \right).
\tag{7}
$$

The tractions of the vector wavefunctions are thus calculated as

$$
\boldsymbol{t}^{(r)} \left(\boldsymbol{\psi}^0_{1\sigma ml}(\boldsymbol{r}) \right) = \mu r \frac{d}{dr} \left(\frac{j_l(k_s r)}{r} \right) \boldsymbol{A}_{1\sigma ml}(\theta, \varphi),
\tag{8}
$$

$$t^{(r)}\left(\boldsymbol{\psi}_{2\sigma ml}^{0}(\boldsymbol{r})\right) = \mu\left[\left(2k_s j_l''(k_s r) + \frac{2j_l'(k_s r)}{r} - \frac{2j_l(k_s r)}{k_s r^2} + k_s j_l(k_s r)\right) \boldsymbol{A}_{2\sigma ml}(\theta, \varphi)\right.$$
$$\left. + 2\sqrt{l(l+1)}\frac{d}{dr}\left(\frac{j_l(k_s r)}{k_s r}\right) \boldsymbol{A}_{3\sigma ml}(\theta, \varphi)\right], \tag{9}$$

$$t^{(r)}\left(\boldsymbol{\psi}_{3\sigma ml}^{0}(\boldsymbol{r})\right) = \mu\left(\frac{k_p}{k_s}\right)^{3/2}\left[\left(2k_p j_l''(k_p r) + \frac{2k_p^2 - k_s^2}{k_p}j_l(k_p r)\right) \boldsymbol{A}_{3\sigma ml}(\theta, \varphi)\right.$$
$$\left. + 2\sqrt{l(l+1)}\frac{d}{dr}\left(\frac{j_l(k_p r)}{k_p r}\right) \boldsymbol{A}_{2\sigma ml}(\theta, \varphi)\right]. \tag{10}$$

Assuming that the sources of the incident wave lie outside the sphere (see Fig. 1), it is possible and convenient to expand the incident wave in terms of the regular spherical vector wavefunctions as

$$\boldsymbol{u}^{in}(\boldsymbol{r}) = \sum_{\tau\sigma ml} b_{\tau\sigma ml}\boldsymbol{\psi}_{\tau\sigma ml}^{0}(\boldsymbol{r}), \tag{11}$$

where the summation is over $\tau = 1, 2, 3$, $\sigma = e, o$, $m = 0, 1, \ldots$ and $l = m, m+1, m+2, \ldots$. This expansion is valid out to the sources of the incident wave. The incident wave is not specified at present, however, the expansion coefficients $b_{\tau\sigma ml}$ are in principle known. The incident wave is scattered by the sphere, thus the outgoing scattered wave must satisfy the radiation conditions and can be expanded in terms of the outgoing spherical vector wavefunctions in the isotropic surrounding

$$\boldsymbol{u}^{sc}(\boldsymbol{r}) = \sum_{\tau\sigma ml} g_{\tau\sigma ml}\boldsymbol{\psi}_{\tau\sigma ml}^{+}(\boldsymbol{r}), \tag{12}$$

where the expansion coefficients $g_{\tau\sigma ml}$ are to be determined. This is done by determining the transition (**T**) matrix, which is defined as the linear relation between the expansion coefficients of the incident and scattered waves

$$g_{\tau\sigma ml} = \sum_{\tau'\sigma'm'l'} T_{\tau\sigma ml,\tau'\sigma'm'l'} b_{\tau'\sigma'm'l'}. \tag{13}$$

Thus, the **T** matrix completely specifies the scattering by the obstacle and is convenient to use when the effective properties in a polycrystalline material are determined. In the next section the transversely isotropic sphere is studied.

3. The transversely isotropic sphere

In this section the material properties of the sphere are defined and necessary relations to determine the displacement field and the traction inside the sphere are explained. The transversely isotropic sphere with density ρ_1 is oriented in such a way that the axis of anisotropy is perpendicular to the xy plane. Therefore, the constitutive relation, which contains five independent stiffness constants, in the Cartesian coordinates is

$$\begin{Bmatrix} \sigma_{xx} \\ \sigma_{yy} \\ \sigma_{zz} \\ \sigma_{xy} \\ \sigma_{yz} \\ \sigma_{zx} \end{Bmatrix} = \begin{bmatrix} C_{11} & C_{12} & C_{13} & 0 & 0 & 0 \\ C_{12} & C_{11} & C_{13} & 0 & 0 & 0 \\ C_{13} & C_{13} & C_{33} & 0 & 0 & 0 \\ 0 & 0 & 0 & C_{11} - C_{12} & 0 & 0 \\ 0 & 0 & 0 & 0 & 2C_{44} & 0 \\ 0 & 0 & 0 & 0 & 0 & 2C_{44} \end{bmatrix} \begin{Bmatrix} \epsilon_{xx} \\ \epsilon_{yy} \\ \epsilon_{zz} \\ \epsilon_{xy} \\ \epsilon_{yz} \\ \epsilon_{zx} \end{Bmatrix}. \tag{14}$$

To be able to apply boundary conditions on the sphere it is useful to apply spherical coordinates, thus the following relation for the transformation of the stress and strain tensor from Cartesian to spherical coordinates is used

$$\mathbf{S}_s = \mathbf{R}^T\mathbf{S}_c\mathbf{R}, \tag{15}$$

where $\mathbf{S}_s$ and $\mathbf{S}_c$ are stress or strain tensors in the spherical and the Cartesian coordinates, respectively, and $\mathbf{R}$ is the rotation matrix with the following appearance

$$\mathbf{R} = \begin{bmatrix} \cos\varphi\sin\theta & \cos\varphi\cos\theta & -\sin\varphi \\ \sin\varphi\sin\theta & \sin\varphi\cos\theta & \cos\varphi \\ \cos\theta & -\sin\theta & 0 \end{bmatrix}. \tag{16}$$

Therefore, considering the definition of the strains in spherical coordinates

$$
\epsilon_{rr} = \frac{\partial u_r}{\partial r}, \quad \epsilon_{\varphi\varphi} = \frac{1}{r\sin\theta}\frac{\partial u_\varphi}{\partial\varphi} + \frac{\cot\theta}{r}u_\theta + \frac{u_r}{r},
$$
$$
\epsilon_{\theta\theta} = \frac{1}{r}\frac{\partial u_\theta}{\partial\theta} + \frac{u_r}{r}, \quad \epsilon_{\theta\varphi} = \frac{1}{2r}\left(\frac{\partial u_\varphi}{\partial\theta} - \cot\theta u_\varphi + \frac{1}{\sin\theta}\frac{\partial u_\theta}{\partial\varphi}\right),
$$
$$
\epsilon_{\varphi r} = \frac{1}{2}\left(\frac{1}{r\sin\theta}\frac{\partial u_r}{\partial\varphi} + \frac{\partial u_\varphi}{\partial r} - \frac{u_\varphi}{r}\right), \quad \epsilon_{r\theta} = \frac{1}{2}\left(\frac{\partial u_\theta}{\partial r} - \frac{u_\theta}{r} + \frac{1}{r}\frac{\partial u_r}{\partial\theta}\right),
$$
(17)

the stress–strain relations in spherical coordinates are derived

$$
\sigma_{rr} = (\alpha_1 + 2\alpha_2)\epsilon_{rr} + \alpha_1\epsilon_{\theta\theta} + (\alpha_1 - \beta_2 + \beta_3)\epsilon_{\varphi\varphi} - 2\beta_1(\epsilon_{rr}\cos 2\theta - \epsilon_{r\theta}\sin 2\theta)
$$
$$
- \beta_3\left(\epsilon_{\varphi\varphi}\cos 2\theta\right) + \beta_2\left((\epsilon_{rr} - \epsilon_{\theta\theta})\cos 4\theta - 2\epsilon_{r\theta}\sin 4\theta\right),
$$
(18)

$$
\sigma_{\theta\theta} = (\alpha_1 + 2\alpha_2)\epsilon_{\theta\theta} + \alpha_1\epsilon_{rr} + (\alpha_1 - \beta_2 + \beta_3)\epsilon_{\varphi\varphi} + 2\beta_1(\epsilon_{\theta\theta}\cos 2\theta + \epsilon_{r\theta}\sin 2\theta)
$$
$$
+ \beta_3\left(\epsilon_{\varphi\varphi}\cos 2\theta\right) + \beta_2\left((\epsilon_{\theta\theta} - \epsilon_{rr})\cos 4\theta + 2\epsilon_{r\theta}\sin 4\theta\right),
$$
(19)

$$
\sigma_{\varphi\varphi} = (\alpha_1 + 2\alpha_2 + 2\beta_1 + \beta_2)\epsilon_{\varphi\varphi} + (\alpha_1 - \beta_2 + \beta_3)(\epsilon_{\theta\theta} + \epsilon_{rr}) + \beta_3((\epsilon_{\theta\theta} - \epsilon_{rr})\cos 2\theta + 2\epsilon_{r\theta}\sin 2\theta),
$$
(20)

$$
\sigma_{r\theta} = 2\alpha_2\epsilon_{r\theta} + \beta_1((\epsilon_{\theta\theta} + \epsilon_{rr})\sin 2\theta) + \beta_3\left(\epsilon_{\varphi\varphi}\sin 2\theta\right) + \beta_2((\epsilon_{\theta\theta} - \epsilon_{rr})\sin 4\theta - 2\epsilon_{r\theta}\cos 4\theta),
$$
(21)

$$
\sigma_{r\varphi} = (2\alpha_2 + \beta_1 - \beta_3)\epsilon_{r\varphi} - (2\beta_2 + \beta_1 - \beta_3)\left(\epsilon_{r\varphi}\cos 2\theta - \epsilon_{\theta\varphi}\sin 2\theta\right),
$$
(22)

$$
\sigma_{\theta\varphi} = (2\alpha_2 + \beta_1 - \beta_3)\epsilon_{\theta\varphi} + (2\beta_2 + \beta_1 - \beta_3)\left(\epsilon_{\theta\varphi}\cos 2\theta + \epsilon_{r\varphi}\sin 2\theta\right),
$$
(23)

where

$$
\alpha_1 = \frac{1}{8}(C_{11} + 6C_{13} + C_{33} - 4C_{44}), \quad \alpha_2 = \frac{1}{8}(C_{11} - 2C_{13} + C_{33} + 4C_{44})
$$
$$
\beta_1 = \frac{1}{4}(C_{11} - C_{33}), \quad \beta_2 = \frac{1}{8}(C_{11} - 2C_{13} + C_{33} - 4C_{44}), \quad \beta_3 = \frac{1}{2}(C_{12} - C_{13}).
$$
(24)

Here, α_1, α_2, β_1, β_2 and β_3 are five new stiffness constants. It is observed from Eqs. (18) to (23) that the transformation of the stress–strain relations to spherical coordinates leads to the appearance of factors containing trigonometric functions with argument 2θ and 4θ. In the isotropic limit when $\beta_i = 0$, $i = 1, 2, 3$, $\alpha_1 = \lambda_1$, $\alpha_2 = \mu_1$, with μ_1 and λ_1 being the Lamé parameters of the isotropic sphere, these trigonometric functions vanish and Eqs. (18) to (23) reduce to the isotropic case.

The general elastodynamic equations of motion are

$$
\frac{\partial\sigma_{rr}}{\partial r} + \frac{1}{r}\frac{\partial\sigma_{r\theta}}{\partial\theta} + \frac{1}{r\sin\theta}\frac{\partial\sigma_{r\varphi}}{\partial\varphi} + \frac{1}{r}\left(2\sigma_{rr} - \sigma_{\theta\theta} - \sigma_{\varphi\varphi} + \cot\theta\sigma_{r\theta}\right) - \rho\frac{\partial^2 u_r}{\partial t^2} = 0,
$$
(25)

$$
\frac{\partial\sigma_{r\theta}}{\partial r} + \frac{1}{r}\frac{\partial\sigma_{\theta\theta}}{\partial\theta} + \frac{1}{r\sin\theta}\frac{\partial\sigma_{\theta\varphi}}{\partial\varphi} + \frac{1}{r}\left(\cot\theta\left(\sigma_{\theta\theta} - \sigma_{\varphi\varphi}\right) + 3\sigma_{r\theta}\right) - \rho\frac{\partial^2 u_\theta}{\partial t^2} = 0,
$$
(26)

$$
\frac{\partial\sigma_{r\varphi}}{\partial r} + \frac{1}{r}\frac{\partial\sigma_{\theta\varphi}}{\partial\theta} + \frac{1}{r\sin\theta}\frac{\partial\sigma_{\varphi\varphi}}{\partial\varphi} + \frac{1}{r}\left(3\sigma_{r\varphi} + 2\cot\theta\sigma_{\theta\varphi}\right) - \rho\frac{\partial^2 u_\varphi}{\partial t^2} = 0.
$$
(27)

The stress relations Eqs. (18) to (23) and the equations of motion Eqs. (25) to (27) can of course be expressed in terms of the displacement components, however, these equations are not given as they become very long. Exactly as the stress–strain relations, these equations have factors containing trigonometric functions with argument 2θ and 4θ.

To solve the system of equations inside the sphere it is convenient to use the vector spherical harmonics and expand the displacement field inside the sphere as

$$
\boldsymbol{u}_1(r, \theta, \varphi) = \sum_{\tau\sigma ml} F_{\tau\sigma ml}(r)\boldsymbol{A}_{\tau\sigma ml}(\theta, \varphi).
$$
(28)

The r dependent coefficients $F_{\tau\sigma ml}(r)$ are expanded in powers of r in such a way that the regularity conditions at $r = 0$ are satisfied

$$
F_{1\sigma ml}(r) = \sum_{j=l, l+2, \dots}^{\infty} f_{1\sigma ml,j}r^j,
$$
(29)

$$
F_{2\sigma ml}(r) = \sum_{j=l-1, l+1, \dots}^{\infty} f_{2\sigma ml,j}r^j,
$$
(30)

$$
F_{3\sigma ml}(r) = \sum_{j=l-1, l+1, \dots}^{\infty} f_{3\sigma ml,j}r^j.
$$
(31)

Here $f_{\tau\sigma ml,j}$ (where $f_{3\sigma m0,-1} = 0$) are unknown coefficients. Relations between these coefficients are obtained by inserting the expansions Eqs. (29) to (31) and Eq. (28) into the equations of motion Eqs. (25) to (27). The orthogonality of the vector spherical harmonics means that an arbitrary vector can be expanded in terms of $\mathbf{A}_{\tau\sigma ml}(\theta, \varphi)$. Thus the equations of motion can be expanded in terms of the vector spherical harmonics

$$\sum_{\tau\sigma ml} H_{\tau\sigma ml}(r)\mathbf{A}_{\tau\sigma ml}(\theta, \varphi) = \mathbf{0}. \tag{32}$$

Here $H_{\tau\sigma ml}(r)$ is found as the scalar product of the vector spherical harmonic and the vector equation of motion. The orthogonality of the vector spherical harmonics means that every $H_{\tau\sigma ml}(r)$ must vanish, thus

$$H_{\tau\sigma ml}(r) = 0 \qquad \text{for all} \quad \tau, \sigma, m, l, \tag{33}$$

which gives recursion relations among the unknown coefficients inside the sphere. The explicit expression for $H_{\tau\sigma ml}(r)$ is complicated in the general case and is therefore not given. However, the factors containing trigonometric functions with argument 2θ and 4θ which appear in the stress–strain relations lead to coupling between different values of l. Thus $H_{\tau\sigma ml}(r)$ contains the expansion coefficients $f_{\tau\sigma ml,j}$, $f_{\tau\sigma ml\pm2,j}$, and $f_{\tau\sigma ml\pm4,j}$ (there is also coupling between different values of j and τ, but this happens also in the isotropic case).

The remaining unknown coefficients $f_{\tau\sigma ml,j}$ of the displacement expansion inside the sphere together with the unknown coefficients $g_{\tau\sigma ml}$ of the scattered wave in the surrounding medium can be found by applying the continuity conditions on the boundary of the sphere. Applying the continuity of the displacements is straightforward since the displacement field inside and outside the sphere are both available in terms of the vector spherical harmonics (Eqs. (11), (12) and (28)), However, to facilitate the application of the traction continuity, the traction inside the sphere needs to be expanded in terms of the vector spherical harmonics

$$\mathbf{t}_1^{(r)}(r, \theta, \varphi) = \sum_{\tau\sigma ml} G_{\tau\sigma ml}(r)\mathbf{A}_{\tau\sigma ml}(\theta, \varphi). \tag{34}$$

Since the vector spherical harmonics constitute a complete orthonormal set, the coefficients $G_{\tau\sigma ml}(r)$ are determined from the inner product of the traction vector and the vector spherical harmonic as

$$G_{\tau\sigma ml}(r) = \int_0^\pi \int_0^{2\pi} \mathbf{t}_1^{(r)}(r, \theta, \varphi) \cdot \mathbf{A}_{\tau\sigma ml}(\theta, \varphi) \sin\theta d\theta \, d\varphi. \tag{35}$$

As in the equations of motion, there is here coupling between different values of l.

All the necessary relations for solving the scattering problem is now at hand, although explicit expressions are not given so far. It is quite possible to solve the problem for intermediate frequencies in this way, but here only the low frequency scattering is investigated in detail. In this case leading order $\mathbf{T}$ matrix elements appear for $l = 0$, $l = 1$ and $l = 2$ and it is possible to give explicit expressions for these. In the following sections this is accomplished with a division depending on the value of $m = 0, 1, 2$.

4. Low frequency T matrix elements for $m = 0$

For the case with $m = 0$ all the fields are φ independent and only contain $\sigma = e$ (see Eq. (6)). Consequently the problem is axisymmetric, and can be viewed as the case when an incident P wave is parallel to the axis of anisotropy. In this specific case when there is no $\sigma = o$ part there is no coupling between SH waves and P-SV waves and they can be studied separately. A study of the incident SH waves for such an axisymmetric problem is performed by the authors and the $\mathbf{T}$ matrix elements are presented [16]. However, the leading order of the $\mathbf{T}$ matrix elements for the SH case behaves as $(ka)^5$ which is higher than the leading order of the P-SV case (as is shown in the following) and is not of the interest in the current study. For the P-SV case the problem is decoupled into two parts for even and odd values of l, which are studied separately.

4.1. Even–even P-SV waves

When $m = 0$ and $\sigma = e$ the following ansatz for the displacement field inside the sphere can be made according to Eq. (28) for even values of l as

$$\begin{aligned} \mathbf{u}_1(r, \theta, \varphi) &= F_{2e02}(r)\mathbf{A}_{2e02}(\theta, \varphi) + F_{2e04}(r)\mathbf{A}_{2e04}(\theta, \varphi) + \ldots \\ &+ F_{3e00}(r)\mathbf{A}_{3e00}(\theta, \varphi) + F_{3e02}(r)\mathbf{A}_{3e02}(\theta, \varphi) + F_{3e04}(r)\mathbf{A}_{3e04}(\theta, \varphi) + \ldots, \end{aligned} \tag{36}$$

where the r dependent coefficients are expanded into a power series in r according to Eqs. (30) and (31)

$$\begin{aligned} F_{2e02}(r) &= f_{2e02,1}r + f_{2e02,3}r^3 + \ldots, \quad F_{2e04}(r) = f_{2e04,3}r^3 + \ldots, \\ F_{3e00}(r) &= f_{3e00,1}r + f_{3e00,3}r^3 + \ldots, \quad F_{3e02}(r) = f_{3e02,1}r + f_{3e02,3}r^3 + \ldots, \quad F_{3e04}(r) = f_{3e04,3}r^3 + \ldots, \end{aligned} \tag{37}$$

With this ansatz of the displacement field the equation of motion can be expanded as in Eq. (32) and the first two coefficients $H_{\tau\sigma ml}$ become

$$H_{3e00} = \frac{4}{7\sqrt{5}} (7\beta_1 + 2\beta_2)\left(\sqrt{6}f_{2e02,1} - 3f_{3e02,1}\right) r + \frac{1}{3}\Big(3\rho_1\omega^2 f_{3e00,1} + f_{3e00,3}(30\alpha_1 + 60\alpha_2 + 20\beta_1 - 2\beta_2)$$
$$+ 32\sqrt{5}\beta_2 f_{2e04,3} - 4\sqrt{5}(7\beta_1 + 2\beta_2)f_{3e02,3} + 64\beta_2 f_{3e04,3} \Big) r^3 + \ldots = 0,$$

$$H_{3e02} = \frac{2}{21}\left(\sqrt{6}f_{2e02,1} - 3f_{3e02,1}\right)(21\alpha_2 + 6\beta_1 - \beta_2)r + \Big(\frac{2}{3}f_{3e02,3}(15\alpha_1 + 21\alpha_2 - 4\beta_1 + 4\beta_2) \tag{38}$$
$$+ 2\sqrt{6}f_{2e02,3}(\beta_2 - \alpha_1) + 8\beta_1 f_{2e04,3} + \frac{272}{33}\beta_2 f_{2e04,3} - \frac{56\beta_1 f_{3e00,3}}{3\sqrt{5}} - \frac{16\beta_2 f_{3e00,3}}{3\sqrt{5}} - \frac{56\beta_1 f_{3e04,3}}{\sqrt{5}}$$
$$+ \frac{112\beta_2 f_{3e04,3}}{33\sqrt{5}} + \rho_1\omega^2 f_{3e02,1} \Big) r^3 + \ldots = 0.$$

Of course it is possible to find more $H_{\tau\sigma ml}$ coefficients, however, they do not lead to extra relations among the $f_{\tau\sigma ml,j}$ coefficients which are explicitly presented in Eq. (37) and those are sufficient to obtain the **T** matrix elements for low frequencies. It then follows from Eq. (38) and the linear independence of the powers of r that

$$f_{3e02,1} = \sqrt{\frac{2}{3}}f_{2e02,1}, \qquad f_{3e04,1} = \frac{2}{\sqrt{5}}f_{2e04,3},$$
$$f_{3e02,3} = \frac{1}{20\sqrt{5}(7\beta_1 + 2\beta_2)}\Big(10f_{3e00,3}(15\alpha_1 + 30\alpha_2 + 10\beta_1 - \beta_2) + 3\left(96\sqrt{5}f_{2e04,3}\beta_2 + 5f_{3e00,1}\rho_1\omega^2\right)\Big),$$
$$f_{2e02,3} = \frac{1}{330\sqrt{6}\,(\alpha_1 - \beta_2)}\Big(110f_{3e02,3}(15\alpha_1 + 21\alpha_2 - 4\beta_1 + 4\beta_2) + 40\,(33\beta_1 + 34\beta_2)f_{2e04,3}, \tag{39}$$
$$- 88\sqrt{5}\,(7\beta_1 + 2\beta_2)f_{3e00,3} + 56\sqrt{5}\,(2\beta_2 - 33\beta_1)f_{3e04,3} + 165\rho_1\omega^2 f_{3e02,1} \Big).$$

These relations reduce the eight unknown expansion coefficients explicitly written in the displacement expansions Eqs. (36) and (37) to four. These are all that are needed to obtain the transition matrix for low frequencies. There is of course no particular problem with including more terms in the displacement components which lead to more equations that are needed for higher frequencies.

Applying continuity of the displacement at $r = a$ gives one equation for each $l = 0, 2, \ldots$ for $\tau = 3$ and one equation for each $l = 2, 4, \ldots$ for $\tau = 2$. Likewise continuity of the traction gives one equation for each $l = 0, 2, \ldots$ for $\tau = 3$ and one equation for each $l = 2, 4, \ldots$ for $\tau = 2$. However, since only the low frequency **T** matrix elements are of interest here, it is sufficient to consider the equations only for $l = 0$ and $l = 2$. Consequently, there are six equations to the lowest order. The unknowns are the scattered field coefficients g_{3e00}, g_{3e02} and g_{2e02} in Eq. (12) and the remaining expansion coefficients inside the sphere $f_{3e00,1}, f_{3e00,3}, f_{2e02,1}, f_{2e04,3}$. Thus, there are six equations and seven unknowns. However, since only the lowest order of the **T** matrix elements is of interest it can be assumed that there is no incident partial wave of order $l = 4$ and continuity of the displacement forces $f_{2e04,3}$ to vanish, so only 6 unknowns remain and the system of equations is complete. Solving the system of equations gives the scattered field unknown coefficients $g_{\tau\sigma ml}$ in terms of the incident field coefficients $b_{\tau\sigma ml}$. Substituting these relations into Eq. (13) provides the **T** matrix elements. In the following sections when determining other **T** matrix elements, the displacement field is similarly expanded only to the necessary orders of l, which are $l = 0$, $l = 1$ and $l = 2$ for the θ dependence and to power 3 of r for the r dependence. Furthermore, when applying the boundary conditions the series expansions of the spherical Bessel and Hankel functions outside the sphere are used.

Solving the mentioned system of equations (which is done with Mathematica), the following leading order **T** matrix elements are derived

$$T_{3e00,3e00} = -\frac{ik_p a}{3}\left((k_p a)^2 - \frac{(k_s a)^2\mu\left(4k_p^2(3\alpha_2 - \beta_1 + 3\beta_2 + \beta_3 - 3\mu) + 3k_s^2(6\alpha_2 - 2\beta_1 + 6\beta_2 + 2\beta_3 + 9\mu)\right)}{4k_p^2 M_0 + 3k_s^2 N_0}\right),$$

$$T_{2e02,3e00} = T_{3e00,2e02} = -2\sqrt{\frac{10}{3}}i(k_s a)^3\sqrt{\frac{k_p}{k_s}}\frac{k_s^2(2\beta_1 + \beta_3)\mu}{4k_p^2 M_0 + 3k_s^2 N_0},$$

$$T_{3e02,3e00} = T_{3e00,3e02} = -\frac{4\sqrt{5}}{3}i(k_p a)^3\frac{k_s^2(2\beta_1 + \beta_3)\mu}{4k_p^2 M_0 + 3k_s^2 N_0},$$

$$T_{2e02,2e02} = -2i(k_s a)^3\frac{k_s^2 M_0}{4k_p^2 M_0 + 3k_s^2 N_0},$$

$$T_{3e02,2e02} = T_{2e02,3e02} = -2\sqrt{\frac{2}{3}}i(k_s a)^3 \sqrt{\frac{k_p}{k_s}} \frac{k_p^2 M_0}{4k_p^2 M_0 + 3k_s^2 N_0},$$

$$T_{3e02,3e02} = -\frac{4}{3}i(k_p a)^3 \frac{k_p^2 M_0}{4k_p^2 M_0 + 3k_s^2 N_0}, \tag{40}$$

where

$$M_0 = 2\alpha_2^2 - 2\beta_1^2 + \beta_1\beta_2 - \beta_2^2 - 2\beta_1\beta_3 + \beta_2\beta_3 + \alpha_1\left(3\alpha_2 - \beta_1 + 3\beta_2 + \beta_3 - 3\mu\right) - 2\beta_1\mu + 5\beta_2\mu - 4\mu^2$$
$$+ \alpha_2\left(\beta_2 + 2\left(\beta_3 + \mu\right)\right), \tag{41}$$

$$N_0 = 2M_0 + \frac{5}{3}\mu\left(9\alpha_1 + 6\alpha_2 + 2\beta_1 - 3\beta_2 + 4\beta_3 + 12\mu\right).$$

Of course in the isotropic limit when $\beta_i = 0$, $i = 1, 2, 3$ and $\alpha_1 = \lambda_1$ and $\alpha_2 = \mu_1$, these elements reduce to those of the isotropic case (given by Boström [28]).

4.2. Even–odd P-SV waves

For the even–odd P-SV waves the ansatz of the displacement inside the sphere is made with odd values of l, and taking into account all the assumptions of the low frequency scattering, only the following terms are needed

$$\boldsymbol{u}_1(r, \theta, \varphi) = F_{2e01}(r)\mathbf{A}_{2e01}(\theta, \varphi) + F_{3e01}(r)\mathbf{A}_{3e01}(\theta, \varphi), \tag{42}$$

where

$$F_{2e01}(r) = f_{2e01,0} + f_{2e01,2}r^2, \quad F_{3e01}(r) = f_{3e01,0} + f_{3e01,2}r^2. \tag{43}$$

Substituting the displacement ansatz into Eq. (32) and taking $H_{2e01} = 0$ together with the linear independence of the powers of r, the following relations among expansion coefficients are found

$$f_{2e01,0} = \sqrt{2}f_{3e01,0}, \qquad f_{3e01,2} = \frac{\sqrt{2}\left(\alpha_1 - \alpha_2\right)f_{2e01,2} - f_{3e01,0}\rho_1\omega^2}{4\alpha_1 + 6\alpha_2 - 2\left(2\beta_1 + \beta_2\right)}. \tag{44}$$

Again considering continuity of displacement and traction for $l = 1$ of $\tau = 2$ and $\tau = 3$ provides 4 equations which are sufficient to find the four unknowns $g_{2e01}, g_{3e01}, f_{2e01,2}$ and $f_{3e01,0}$ and the $\mathbf{T}$ matrix elements are determined as

$$T_{2e01,2e01} = -\frac{2}{9}i\left(k_s a\right)^3\left(1 - \frac{\rho_1}{\rho}\right),$$

$$T_{3e01,2e01} = T_{2e01,3e01} = -\frac{\sqrt{2}}{9}i\sqrt{k_p^3 k_s^3}a^3\left(1 - \frac{\rho_1}{\rho}\right), \tag{45}$$

$$T_{3e01,3e01} = -\frac{1}{9}i\left(k_p a\right)^3\left(1 - \frac{\rho_1}{\rho}\right).$$

As is to be expected these elements are identical to those of an isotropic sphere. This is because $l = 1$ corresponds to a rigid body translation at low frequencies so these elements should only depend on the density of the sphere, not on the stiffness properties of the sphere.

5. Low frequency T matrix elements for $m = 1$

In this section the scattering for $m = 1$ is examined. Here, unlike $m = 0$, the elastic waves can be even or odd with respect to φ ($\sigma = e$ and $\sigma = o$) and as for $m = 0$, they can also be even or odd with respect to θ with even and odd values of l. Therefore the problem is decoupled into four parts, even–even, odd–even, even–odd and odd–odd with respect to φ and θ, respectively. Furthermore, the appearance of the even and odd waves with respect to φ and the anisotropy nature of the sphere lead to coupling between different parities of the P-SV waves and the SH waves. This can be observed in Eqs. (2) to (6) where the displacement field in each direction (r, θ, φ) has the same parity with respect to θ and φ, if the P-SV waves ($\boldsymbol{\psi}_{2\sigma ml}$ and $\boldsymbol{\psi}_{3\sigma ml}$) have different parity compared to the SH waves ($\boldsymbol{\psi}_{1\sigma ml}$) with respect to both θ (l values) and φ (σ values). However, the parity of the waves with respect to φ (σ values) does not affect the $\mathbf{T}$ matrix elements when the same values of l and m are considered. Therefore the $\mathbf{T}$ matrix is the same for even–even and odd–even cases and it is the same for even–odd and odd–odd cases as well. Considering this, the derivation of the low frequency $\mathbf{T}$ matrix elements is only explained for the even–even and even–odd parts.

5.1. Even–even P-SV waves and odd–odd SH waves

For this case the already truncated ansatz (expansion to $l_{max} = 2$ at low frequencies) of the displacement field is

$$\boldsymbol{u}_1(r, \theta, \varphi) = F_{1o11}(r)\mathbf{A}_{1o11}(\theta, \varphi) + F_{2e12}(r)\mathbf{A}_{2e12}(\theta, \varphi) + F_{3e12}(r)\mathbf{A}_{3e12}(\theta, \varphi), \tag{46}$$

where the r dependent coefficients are expanded in a power series in r based on Eqs. (29) to (31) (truncation to power 3 in r)

$$\begin{aligned}
F_{1o11}(r) &= f_{1o11,1}r + f_{1o11,3}r^3, \\
F_{2e12}(r) &= f_{2e12,1}r + f_{2e12,3}r^3, \\
F_{3e12}(r) &= f_{3e12,1}r + f_{3e12,3}r^3.
\end{aligned} \tag{47}$$

In the same way as in the previous section, the following recurrence relations among the unknown coefficients can be obtained from Eq. (32)

$$\begin{aligned}
f_{2e12,1} &= \sqrt{\frac{3}{2}}f_{3e12,1}, \\
f_{1o11,1} &= \frac{-1}{6\rho_1\omega^2}\left(6f_{1o11,3}(10\alpha_2 + \beta_1 - \beta_3) - 4\sqrt{15}(2\beta_1 + \beta_3)f_{2e12,3} + 3\sqrt{10}(9\beta_1 + 2\beta_2 + \beta_3)f_{3e12,3}\right), \\
f_{2e12,3} &= \frac{\sqrt{3}\left(5f_{3e12,3}(10\alpha_1 + 14\alpha_2 + \beta_1 - 6\beta_2 + \beta_3) + \sqrt{10}(5\beta_1 + 2\beta_2 - \beta_3)f_{1o11,3} + 5\rho_1\omega^2 f_{3e12,1}\right)}{10\sqrt{2}(3\alpha_1 + \beta_2 + \beta_3)}.
\end{aligned} \tag{48}$$

These relations reduce the total number of unknowns to six which are $g_{1o11}, g_{2e12}, g_{3e12}f_{3e12,1}, f_{2e12,3}$ and $f_{1o11,3}$, and these can be found from the six equations at hand from the continuity of the traction and displacement at the boundary of the sphere for $l = 1$ and $\tau = 1$, $l = 2$ and $\tau = 2$ and $l = 2$ and $\tau = 3$. Solving the system of equations the following leading order **T** matrix elements (which are the same as for the case with the same values of m and l but $\sigma = o$) are derived

$$\begin{aligned}
T_{2\sigma 12, 2\sigma 12} &= -2i(k_s a)^3 \frac{k_s^2 M_1}{4k_p^2 M_1 + 3k_s^2 N_1}, \\
T_{3\sigma 12, 2\sigma 12} &= T_{2\sigma 12, 3\sigma 12} = -2\sqrt{\frac{2}{3}}i(k_s a)^3 \sqrt{\frac{k_p}{k_s}} \frac{k_p^2 M_1}{4k_p^2 M_1 + 3k_s^2 N_1}, \\
T_{3\sigma 12, 3\sigma 12} &= -\frac{4}{3}i(k_p a)^3 \frac{k_p^2 M_1}{4k_p^2 M_1 + 3k_s^2 N_1},
\end{aligned} \tag{49}$$

where

$$M_1 = \alpha_2 - \beta_2 - \mu = C_{44} - \mu, \qquad N_1 = 2M_1 + 5\mu = 2C_{44} + 3\mu, \qquad \sigma = e \text{ or } o. \tag{50}$$

The other **T** matrix elements ($T_{1\sigma 11, 1\sigma 11}, T_{1\sigma 11, 2\sigma' 12}, T_{2\sigma' 12, 1\sigma 11}, T_{1\sigma 11, 3\sigma' 12}$ and $T_{3\sigma' 12, 1\sigma 11}$, where $\sigma' \neq \sigma$) all involve the SH waves and are of the order $(k_s a)^5$ for low frequencies. Thus they are of higher order than the leading order in the low frequency limit $((ka)^3)$ and are not of interest here. Generally all **T** matrix elements which involve the SH waves are at least of order $(k_s a)^5$ and all of them can be neglected in the low frequency limit. Therefore, in the following sections only the **T** matrix elements of the P-SV waves are presented.

5.2. Odd–odd P-SV waves even–even SH waves

For this part the proper ansatz which is already truncated according to the low frequency limit is

$$\mathbf{u}(r, \theta, \varphi) = F_{1e12}(r)\mathbf{A}_{1e12}(\theta, \varphi) + F_{2o11}(r)\mathbf{A}_{2o11}(\theta, \varphi) + F_{3o11}(r)\mathbf{A}_{3o11}(\theta, \varphi). \tag{51}$$

where

$$\begin{aligned}
F_{1e12}(r) &= f_{1e12,2}r^2, \\
F_{2o11}(r) &= f_{2o11,0} + f_{2o11,2}r^2, \\
F_{3o11}(r) &= f_{3o11,0} + f_{3o11,2}r^2.
\end{aligned} \tag{52}$$

The recurrence relations follow in usual way

$$\begin{aligned}
f_{2o11,0} &= \sqrt{2}f_{3o11,0}, \\
f_{2o11,2} &= \frac{\sqrt{30}(\beta_1 + 2\beta_2 - 3\beta_3)f_{1e12,2} + 6\rho_1\omega^2 f_{3o11,0} + 6(4\alpha_1 + 6\alpha_2 + 5\beta_1 + \beta_3)f_{3o11,2}}{3\sqrt{2}(2\alpha_1 - 2\alpha_2 - \beta_1 - 2\beta_2 + 3\beta_3)}.
\end{aligned} \tag{53}$$

Using these and the boundary conditions the **T** matrix elements become

$$T_{2\sigma11,2\sigma11} = -\frac{2}{9}i\,(k_sa)^3\left(1 - \frac{\rho_1}{\rho}\right),$$

$$T_{3\sigma11,2\sigma11} = T_{2\sigma11,3\sigma11} = -\frac{\sqrt{2}}{9}i\sqrt{k_p^3k_s^3}a^3\left(1 - \frac{\rho_1}{\rho}\right), \tag{54}$$

$$T_{3\sigma11,3\sigma11} = -\frac{1}{9}i\left(k_pa\right)^3\left(1 - \frac{\rho_1}{\rho}\right).$$

where $\sigma = e$ or o. As mentioned, $l = 1$ corresponds to rigid body translation at low frequencies and consequently the transition matrix elements only depend on the density of the sphere. These elements are in fact the same as given above in Eq. (45) for $m = 0$ and $l = 1$.

6. Low frequency T matrix elements for $m = 2$

As for $m = 1$ the scattering problem for $m = 2$ can be decoupled into four parts. However, considering the necessary condition $l \geq m$ for the vector spherical harmonics, the smallest possible odd value of l is $l = 3$, which as explained above, lead to higher order of the **T** matrix elements than $(ka)^3$. Therefore, the only interesting value of l is $l = 2$. Considering the coupling between even P-SV waves and odd SH waves and visa versa the problem can be considered for the cases that the P-SV waves are of the order $l = 2$ and the case with the SH waves of the order $l = 2$. However, it is observed that the **T** matrix elements of the SH waves are of order $(k_sa)^5$ and higher which are not of interest. Therefore, only P-SV waves of the order $l = 2$ remains, which of course can be either odd or even with respect to φ, and both cases lead to the same **T** matrix elements. Thus, only the even–even P-SV waves case is investigated.

6.1. Even–even P-SV waves odd–odd SH waves

The suitable displacement ansatz for the coupled even–even P-SV waves and odd–odd SH waves is

$$\boldsymbol{u}_1(r, \theta, \varphi) = F_{1o23}(r)\mathbf{A}_{1o23}(\theta, \varphi) + F_{2e22}(r)\mathbf{A}_{2e22}(\theta, \varphi) + F_{3e22}(r)\mathbf{A}_{3e22}(\theta, \varphi). \tag{55}$$

Here $l = 3$ is included in the ansatz only to show the coupling between SH and P-SV waves. The r dependence coefficients of the Eq. (55) can be expanded as

$$F_{1o23}(r) = f_{1o23,3}r^3,$$

$$F_{2e22}(r) = f_{2e22,1}r + f_{2e22,3}r^3, \tag{56}$$

$$F_{3e22}(r) = f_{3e22,1}r + f_{3e22,3}r^3.$$

As above this gives recursion relations among the unknown coefficients

$$f_{2e22,1} = \sqrt{\frac{3}{2}}f_{3e22,1}, \qquad f_{2e22,3} = \frac{6\left(5\alpha_1 + 7\alpha_2 + 6\beta_1 + 2\beta_3\right)f_{3e22,3} + 4\sqrt{21}\beta_3f_{1o23,3} + 3\rho_1\omega^2f_{3e22,1}}{2\sqrt{6}\left(3\alpha_1 - 3\beta_2 + 4\beta_3\right)}. \tag{57}$$

These relations reduce the number of unknown coefficients inside the sphere to three and together with the three unknown coefficients of the scattered wave there is a total of six unknowns. With the six continuity equations the system of equations can be solved for the **T** matrix elements

$$T_{2\sigma22,2\sigma22} = -2i\,(k_sa)^3\,\frac{k_s^2M_2}{4k_p^2M_2 + 3k_s^2N_2},$$

$$T_{3\sigma22,2\sigma22} = T_{2\sigma22,3\sigma22} = -2\sqrt{\frac{2}{3}}i\,(k_sa)^3\,\sqrt{\frac{k_p}{k_s}}\,\frac{k_p^2M_2}{4k_p^2M_2 + 3k_s^2N_2}, \tag{58}$$

$$T_{3\sigma22,3\sigma22} = -\frac{4}{3}i\left(k_pa\right)^3\,\frac{k_p^2M_2}{4k_p^2M_2 + 3k_s^2N_2},$$

where

$$M_2 = \alpha_2 + \beta_1 + \beta_2 - \beta_3 - \mu = \frac{1}{2}(C_{11} - C_{12}) - \mu, \qquad N_2 = 2M_2 + 5\mu = C_{11} - C_{12} + 3\mu, \qquad \sigma = e \text{ or } o. \tag{59}$$

7. Distribution of inclusions

In this section a random distribution of spherical inclusions of equal size which are randomly oriented is considered and phase velocity and attenuation of plane P and S waves are calculated approximately for low frequencies. This can be

a model of the grain scattering in a polycrystalline material, typically a metal, but this model is also valid for a particle composite. To deal with this problem the simple theory of Foldy [3] is used. In this theory the multiple scattering between the inclusions is neglected, therefore its validity is generally limited to low volume concentrations of inclusions. However, in the low frequency limit each grain scatters extremely little and neglect of the multiple scattering should be valid even for a high concentration of inclusions. In this simple approximation the effective complex wave number K is related to the forward scattered amplitude by the equation

$$K_i^2 = k_i^2 + 4\pi N \bar{f}_i, \tag{60}$$

where the index i can be P or S for longitudinal and transverse waves, respectively, k is the wave number of the matrix, N is the number density of inclusions and $\bar{f}_i$ is the average (over all orientations of incidence) forward scattering amplitude which can be calculated from the **T** matrix elements as [5]

$$\bar{f}_p = -\frac{i}{k_p} \sum_{\sigma ml} T_{3\sigma ml, 3\sigma ml}, \tag{61}$$

for the average forward scattering of P waves and

$$\bar{f}_s = -\frac{i}{2k_s} \sum_{\substack{\tau\sigma ml \\ \tau=1,2}} T_{\tau\sigma ml, \tau\sigma ml}, \tag{62}$$

for the average forward scattering of S waves. For low frequencies only the **T** matrix elements calculated explicitly in the previous sections need to be included in the sums. Substituting Eqs. (61) and (62) into Eq. (60) the following equations are obtained for calculating the effective wave numbers

$$\begin{aligned}
\left(\frac{K_p}{k_p}\right)^2 &= 1 - \frac{4\pi id}{Vk_p^3} \sum_{\sigma ml} T_{3\sigma ml, 3\sigma ml}, \\
\left(\frac{K_s}{k_s}\right)^2 &= 1 - \frac{2\pi id}{Vk_s^3} \sum_{\substack{\tau\sigma ml \\ \tau=1,2}} T_{\tau\sigma ml, \tau\sigma ml},
\end{aligned} \tag{63}$$

where $V = 4\pi a^3/3$ is the volume of a single grain and d is the relative density of grains. The phase velocity and attenuation of the material are related to the real and imaginary parts of the effective wave number as

$$\begin{aligned}
\frac{\alpha_i}{k_i} &= \operatorname{Im} \frac{K_i}{k_i}, \\
\frac{C_i}{c_i} &= \operatorname{Re} \frac{k_i}{K_i},
\end{aligned} \tag{64}$$

where c_i is the phase velocity in the matrix, C_i is the effective velocity and α_i is the attenuation.

However, in the low frequency limit the leading order terms of the **T** matrix are all imaginary, see the previous sections. To obtain the attenuation also the leading order real part of the **T** matrix elements are needed. These can be obtained from the "hermitian" property of the **T** matrix [29]

$$\mathbf{T}^\dagger \cdot \mathbf{T} = -\operatorname{Re}\mathbf{T}. \tag{65}$$

where the "dagger" means the Hermitian conjugate. Summarizing, by doing all the indicated calculations it is possible to obtain an explicit form of the effective wave numbers Eq. (63)

$$\begin{aligned}
\left(\frac{K_p}{k_p}\right)^2 &= 1 + A_p + B_p i, \\
\left(\frac{K_s}{k_s}\right)^2 &= 1 + A_s + B_s i,
\end{aligned} \tag{66}$$

where the coefficients are real and given by

$$\begin{aligned}
A_p = -\frac{1}{9}\Bigg[&\frac{36M_0 k_p^2}{4M_0 k_p^2 + 3N_0 k_s^2} + \frac{72M_1 k_p^2}{4M_1 k_p^2 + 3N_1 k_s^2} + \frac{72M_2 k_p^2}{4M_2 k_p^2 + 3N_2 k_s^2} + \frac{9(\rho - \rho_1)}{\rho} \\
&+ 9\left(1 - \frac{\mu k_s^2 \left(4k_p^2(3\alpha_2 - \beta_1 + 3\beta_2 + \beta_3 - 3\mu) + 3k_s^2(6\alpha_2 - 2\beta_1 + 6\beta_2 + 2\beta_3 + 9\mu)\right)}{k_p^2\left(4M_0 k_p^2 + 3N_0 k_s^2\right)}\right)\Bigg],
\end{aligned}$$

$$B_p = \frac{(k_p a)^3}{9} \left[\frac{(\rho_1 - \rho)^2}{\rho^2} \left(1 + 2\frac{k_s^3}{k_p^3}\right) + \frac{24\left(2M_0^2 k_p^5 + 3M_0^2 k_s^5 + 10\left(2\beta_1 + \beta_3\right)^2 \mu^2 k_p k_s^4\right)}{k_p \left(4M_0 k_p^2 + 3N_0 k_s^2\right)^2} + \frac{48M_1^2 \left(2k_p^5 + 3k_s^5\right)}{k_p \left(4M_1 k_p^2 + 3N_1 k_s^2\right)^2} \right.$$

$$+ \frac{3}{\left(4M_0 k_p^2 + 3N_0 k_s^2\right)^2} \left(120\left(2\beta_1 + \beta_3\right)^2 \mu^2 \frac{k_s^9}{k_p^5} + \left[4M_0 k_p^2 + k_s^2 \left(3N_0 - 4\mu\left(3\alpha_2 - \beta_1 + 3\beta_2 + \beta_3 - 3\mu\right)\right) \right.\right.$$

$$\left.\left. - 3\mu\frac{k_s^4}{k_p^2}\left(6\alpha_2 - 2\beta_1 + 6\beta_2 + 2\beta_3 + 9\mu\right) \right]^2 + 80\left(2\beta_1 + \beta_3\right)^2 \mu^2 k_s^4 \right) + \frac{48M_2^2\left(2k_p^5 + 3k_s^5\right)}{k_p\left(4M_2 k_p^2 + 3N_2 k_s^2\right)^2} \right],$$

$$A_s = -\frac{1}{9}\left(\frac{27M_0 k_s^2}{4M_0 k_p^2 + 3N_0 k_s^2} + \frac{54M_1 k_s^2}{4M_1 k_p^2 + 3N_1 k_s^2} + \frac{54M_2 k_s^2}{4M_2 k_p^2 + 3N_2 k_s^2} + \frac{9\left(\rho - \rho_1\right)}{\rho} \right),$$

$$B_s = \frac{1}{9}(k_s a)^3 \left[\frac{18\left(2M_0^2 k_p^5 + 3M_0^2 k_s^5 + 10\left(2\beta_1 + \beta_3\right)^2 \mu^2 k_p k_s^4\right)}{k_s\left(4M_0 k_p^2 + 3N_0 k_s^2\right)^2} + \frac{36M_1^2\left(2k_p^5 + 3k_s^5\right)}{k_s\left(4M_1 k_p^2 + 3N_1 k_s^2\right)^2} \right.$$

$$\left. + \frac{36M_2^2\left(2k_p^5 + 3k_s^5\right)}{k_s\left(4M_2 k_p^2 + 3N_2 k_s^2\right)^2} + \frac{(\rho_1 - \rho)^2}{\rho^2}\left(\frac{k_p^3}{k_s^3} + 2\right) \right].$$

$$(67)$$

In the low frequency limit the parameters A_i and B_i are small so the explicit form of the normalized attenuation and phase velocity can with good accuracy be calculated as

$$\frac{\alpha_i}{k_i} = \frac{B_i}{2},$$

$$\frac{c_i}{C_i} = 1 + \frac{A_i}{2}.$$

$$(68)$$

Here it is observed that for low frequencies the attenuation coefficients are dependent on the forth power of frequency (or wave number) while the phase velocities are independent of frequency.

8. Numerical results for polycrystalline materials

In this section the results from the previous section are applied to transversely isotropic (also called hexagonal) polycrystalline materials. To verify the present results comparisons are made with Yang et al. [19] and recent FE computations by Huang and Lowe [30], the latter only for P waves. Yang et al. [19] use a volume integral equation method together with a statistical approach with a two-point correlation function (TCP) to estimate the attenuation (this method has later been refined to a generalized TCP to better model the grain distribution in FEM, see [25]).

In FEM, single phase polycrystals are considered, so the individual grains of each model have the same mass density and elastic constants. Also, the grains within each model are defined with uniformly randomly oriented crystallographic axes, making the model macroscopically homogeneous and isotropic [21,22]. These assumptions are the same as in the present method. The FEM methodology is described in detail by Pamel et al. [22], where different aspects regarding background theory, grain generation, finite element spatial discretization, material model, loading and boundary conditions for the FE model are addressed. The developed FE model is used to study wave propagation in polycrystalline materials with cubic symmetry [23] and for general anisotropy [25] and exactly the same method (with the same grains, mesh, etc.) are used in the FE result reported here [30]. Suitable adaptations of already developed analytical methods in order to compare with FE results are also discussed in these studies. Several important issues regarding the FE model, such as determination of effective media parameters, estimating modeling errors and uncertainties and better incorporating FE model information into theoretical models are investigated by Huang et al. [26]. When comparing the FE results with the present method the normalization is performed so that the mean grain volume in FEM determines the sphere radius (assuming spherical grains) in the present method.

For a polycrystalline material the grains are filling the whole volume so the relative density of grains is chosen as $d = 1$. This means that the spherical grains must be overlapping, but this does not matter at low frequencies where the volume of the grains determines the scattering and it is important to get the volume that scatters correct. When the grains fill the whole volume the question is how to choose the surrounding isotropic material when considering the scattering by one grain. For the density this is simple as it is the same everywhere, so in the notation from previous sections $\rho = \rho_1$, and then some terms vanish in the expressions giving the attenuation and phase velocity. As is customary in this context the Lamé constants are chosen as the Voigt averages [17,19]

$$\lambda = \frac{1}{15}(C_{11} + 5C_{12} + C_{33} + 8C_{13} - 4C_{44}),$$

$$\mu = \frac{1}{30}(7C_{11} - 5C_{12} + 2C_{33} - 4C_{13} + 12C_{44}).$$

$$(69)$$

Table 1
Table of materials properties [31].

Material properties											
	Elasticity constants (Gpa)					Density (g/cm³)	Anisotropy factor			Phase velocity	
	C_{11}	C_{12}	C_{13}	C_{33}	C_{44}	ρ	γ_{100}	γ_{010}	γ_{001}	C_p/c_p	C_s/c_s
Ti	162	92	69	180	47	4.54	1.01	0.84	1.34	0.9971	0.9920
Zn	179	37	55	69	46	7.14	0.74	6.57	0.64	0.9674	0.9594
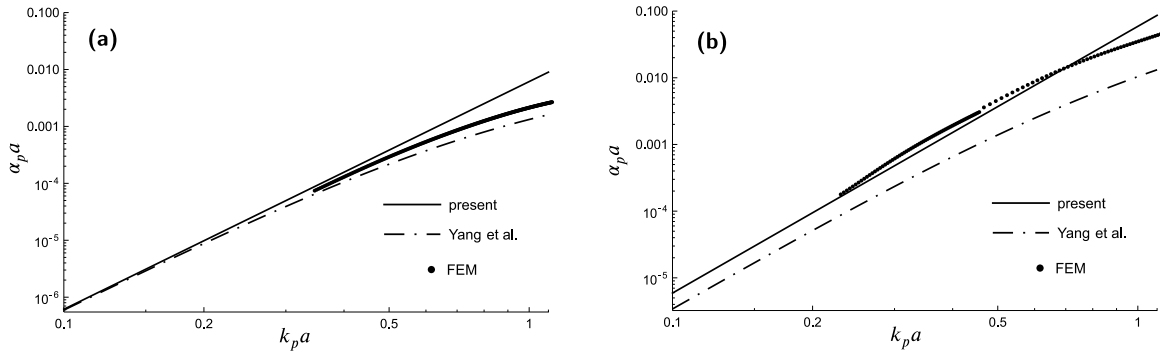
Fig. 2. Normalized longitudinal attenuation $\alpha_p a$ with respect to normalized frequency $k_p a$ evaluated by the present method (solid line), the method presented in Yang et al. (2011) (dashed line) and FEM (dots), for (**a**) titanium and (**b**) zinc.

It is noted that these are different from the α_1 and α_2 defined in Eq. (24) contrary to the situation in 2D [27]. To measure the anisotropy of a transversely isotropic material the following degrees of anisotropy are introduced [19]

$$\gamma_{100} = 2C_{44}/(C_{11} - C_{13}), \qquad \gamma_{010} = 2C_{44}/(C_{33} - C_{13}), \qquad \gamma_{001} = 2C_{44}/(C_{11} - C_{12}), \tag{70}$$

which are all equal to 1 in the case of isotropy.

In the following, the attenuation and phase velocity are calculated for two different transversely isotropic materials with different degrees of anisotropy. Table 1 shows the elasticity properties of titanium and zinc with their degrees of anisotropy. From the degrees of anisotropy it is seen that titanium is rather weakly anisotropic, while zinc can be considered a strongly anisotropic material. Phase velocities of titanium and zinc are also presented in Table 1 and it is noted that with the present method they are independent of frequency for low frequencies. The normalized longitudinal phase velocity evaluated with the present method is 0.9971 and 0.9674 for titanium and zinc, respectively. This is in good agreement with the ones derived with FEM for low frequencies, which are 0.9970 and 0.9632 for titanium and zinc, respectively.

Turning to attenuation, Fig. 2 shows the normalized longitudinal attenuation $\alpha_p a$ with respect to normalized frequency $k_p a$ evaluated by the present method (solid line), the method presented in Yang et al. [19] (dashed line) and FEM (dots) for (a) titanium and (b) zinc. In Fig. 2(b) it can be observed that the present method has a much better agreement with FEM for low frequencies in comparison with Yang et al. [19] for zinc with higher degrees of anisotropy. Defining the error as $|\alpha - \alpha_{FEM}|/\alpha_{FEM}$, Fig. 3 shows the error for longitudinal attenuation with respect to normalized frequency $k_p a$ evaluated for the present method (solid line) and the method presented in Yang et al. [19] (dashed line) for (a) titanium and (b) zinc. Specifically, for zinc at the lowest frequency $k_p a \approx 0.21$ of the FEM calculations, the present method has a 7% error while the Yang et al. [19] error is 51%. The figure also shows that the present method is only valid for low frequencies, up to around $k_p a = 0.5$ the correspondence with the FE results is very good. It is noticed that the FE curve for zinc has a jump 5.7% at $k_p a = 0.46$ and this is due to a change of mesh [26]. This is of course an indication of the inaccuracies that occur in the FE results.
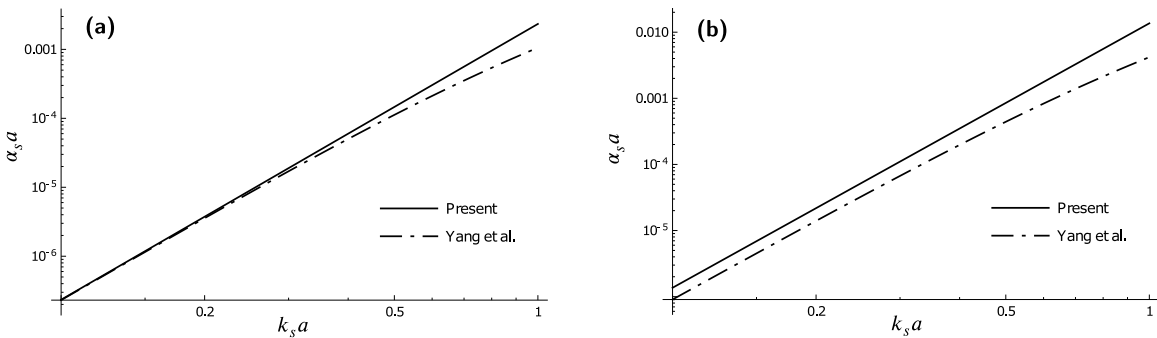
The normalized transverse attenuation is presented in Fig. 4 in the same manner (but without any FE results). For the low degrees of anisotropy of titanium the correspondence between the two methods is good for low frequencies, but the difference becomes substantial when the degrees of anisotropy become large for zinc.

9. Concluding remarks

In the present paper the scattering by a transversely isotropic sphere in an isotropic surrounding is investigated. The focus is on calculating the elements of the transition matrix for low frequencies and these are obtained in explicit form. This is then applied to calculate the attenuation and phase velocity for low frequencies in a material with many randomly oriented spheres using the simple theory of Foldy. As an application, the attenuation and phase velocity is computed for polycrystalline titanium and zinc assuming randomly oriented grains. Comparisons are performed with the theory of Yang
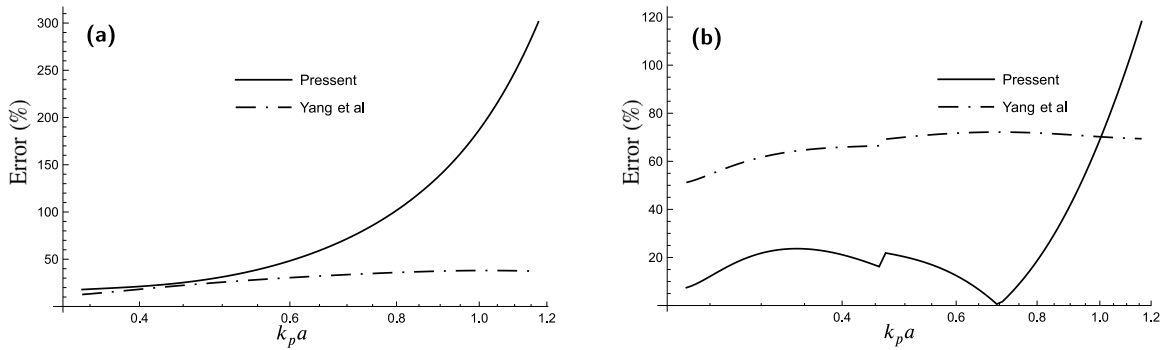
Fig. 3. Error of longitudinal attenuation ($|\alpha - \alpha_{FEM}|/\alpha_{FEM}$) with respect to normalized frequency ($k_p a$) for the present method (solid line) and the method presented in Yang et al. (2011) (dashed line), for (**a**) titanium and (**b**) zinc.

Fig. 4. Normalized transverse attenuation ($\alpha_s a$) with respect to normalized frequency ($k_s a$) evaluated by the present method (solid line) and the method presented in Yang et al. (2011) (dashed line), for (**a**) titanium and (**b**) zinc.

et al. [19] and also by recent FE computations by Huang and Lowe [30]. For low frequencies the correspondence with FEM is very good but particularly for the stronger anisotropy for zinc the correspondence with Yang et al. [19] is rather poor (but as opposed to the present approach, the results of Yang et al. [19] are not limited to low frequencies).

The present approach is limited to low frequencies due to several factors. The **T** matrix elements are only given to leading order, however, there is no particular problem to compute more elements to desired accuracy, see [16], but this then becomes a numerical approach without the possibility to give explicit formulas. Use of the Foldy theory means that multiple scattering is neglected, this can partly by improved by using more refined theories for multiple scattering. The present approach is also limited to spherical grains, at low frequencies this should not matter, but for higher frequencies this is questionable. All in all it seems difficult, and probably not worthwhile, to extend the present approach to higher frequencies.

The present results can naturally be generalized in various directions. Other classes of anisotropy are of course of interest, and these are more challenging as the materials then possess no axis of rotationally symmetry. The simplest such case is a cubic material and work on this has in fact been started. In the present paper only spheres of the same size and type are considered. There seems to be no particular problem with investigating also a size distribution or spheres of different materials, a duplex material for instance.

CRediT authorship contribution statement

Ata Jafarzadeh: Methodology, Software, Formal analysis, Writing – original draft. **Peter D. Folkow:** Methodology, Writing – review & editing, Supervision, Funding acquisition. **Anders Boström:** Conceptualization, Methodology, Writing – review & editing, Supervision, Funding acquisition.

Declaration of competing interest

Acknowledgments

The FE results that are used as a comparison have very kindly been provided by Prof. M. Lowe and Dr. M. Huang, Imperial College, London.

References

[1] A. de Hoop, Handbook of radiation and scattering of waves: acoustic waves in fluids, elastic waves in solids, electromagnetic waves, Academic Press, San Diego, 1995.

[2] V. Varadan, A. Lakhtakia, V. Varadan, Field Representations and Introduction to Scattering, North-Holland, Amsterdam, 1991.

[3] L.L. Foldy, The multiple scattering of waves. I. General theory of isotropic scattering by randomly distributed scatterers, Phys. Rev. 67 (3–4) (1945) 107–119, http://dx.doi.org/10.1103/PhysRev.67.107.

[4] S. Datta, H. Ledbetter, Y. Shindo, A. Shah, Phase velocity and attenuation of plane elastic waves in a particle-reinforced composite medium, Wave Motion 10 (2) (1988) 171–182, http://dx.doi.org/10.1016/0165-2125(88)90042-X.

[5] A. Boström, P. Olsson, S.K. Datta, Effective plane wave propagation through a medium with spheroidal inclusions surrounded by thin interface layers, Mech. Mater. 14 (1) (1992) 59–66, http://dx.doi.org/10.1016/0167-6636(92)90018-9.

[6] C. Wan, H. Li, Analytical method and semianalytical method for analysis of scattering by anisotropic sphere: A review, Int. J. Antennas Propag. 2012 (2012) 782320, http://dx.doi.org/10.1155/2012/782320.

[7] A. Doicu, Null-field method to electromagnetic scattering from uniaxial anisotropic particles, Opt. Commun. 218 (2003) 11–17, http://dx.doi.org/10.1016/S0030-4018(03)01164-7.

[8] J. Wang, Y. Han, L. Han, Z. Cui, Electromagnetic scattering from gyroelectric anisotropic particle by the T-matrix method, J. Quant. Spectrosc. Radiat. Transfer 135 (2014) 20–29, http://dx.doi.org/10.1016/j.jqsrt.2013.12.009.

[9] P. Martin, J. Berger, Waves in wood: free vibrations of a wooden pole, J. Mech. Phys. Solids 49 (2001) 1155–1178, http://dx.doi.org/10.1016/S0022-5096(00)00068-5.

[10] S. Hasheminejad, M. Maleki, Acoustic resonance scattering from a submerged anisotropic sphere, Acoust. Phys. 54 (2008) 168–179, http://dx.doi.org/10.1134/S1063771008020048.

[11] A. Norris, A. Shuvalov, Elastodynamics of radially inhomogeneous spherically anisotropic elastic materials in the Stroh formalism, Proc. Math. Phys. Eng. Sci. 468 (2012) 467–484, http://dx.doi.org/10.1098/rspa.2011.0463.

[12] M. Guild, A. Alù, M. Haberman, Cloaking of an acoustic sensor using scattering cancellation, Appl. Phys. Lett. 105 (2014) 023510, http://dx.doi.org/10.1063/1.4890614.

[13] M. Chung, Stress amplification/shielding phenomena of spherically anisotropic and radially inhomogeneous linear elastic hollow spheres, Q. J. Mech. Appl. Math. 72 (2019) 535–544, http://dx.doi.org/10.1093/qjmam/hbz017.

[14] A. Boström, Scattering by an anisotropic circle, Wave Motion 57 (2015) 239–244, http://dx.doi.org/10.1016/j.wavemoti.2015.04.007.

[15] A. Boström, Scattering of in-plane elastic waves by an anisotropic circle, Q. J. Mech. Appl. Math. 71 (2018) 139–155, http://dx.doi.org/10.1093/qjmam/hbx029.

[16] A. Jafarzadeh, P.D. Folkow, A. Boström, Scattering of elastic SH waves by transversely isotropic sphere, in: Proceedings of the International Conference on Structural Dynamic, Vol. 2, EURODYN, 2020, pp. 2782–2797, http://dx.doi.org/10.47964/1120.9228.18744.

[17] F.E. Stanke, G.S. Kino, A unified theory for elastic wave propagation in polycrystalline materials, J. Acoust. Soc. Am. 75 (3) (1984) 665–681, http://dx.doi.org/10.1121/1.390577.

[18] R.B. Thompson, F. Margetan, P. Haldipur, L. Yu, A. Li, P. Panetta, H. Wasan, Scattering of elastic waves in simple and complex polycrystals, Wave Motion 45 (5) (2008) 655–674, http://dx.doi.org/10.1016/j.wavemoti.2007.09.008.

[19] L. Yang, O. Lobkis, S. Rokhlin, Explicit model for ultrasonic attenuation in equiaxial hexagonal polycrystalline materials, Ultrasonics 51 (3) (2011) 303–309, http://dx.doi.org/10.1016/j.ultras.2010.10.002.

[20] J. Li, S. Rokhlin, Elastic wave scattering in random anisotropic solids, Int. J. Solids Struct. 78 (2016) 110–124, http://dx.doi.org/10.1016/j.ijsolstr.2015.09.011.

[21] A. Van Pamel, C.R. Brett, P. Huthwaite, M. Lowe, Finite element modelling of elastic wave scattering within a polycrystalline material in two and three dimensions, J. Acoust. Soc. Am. 138 (4) (2015) 2326–2336, http://dx.doi.org/10.1121/1.4931445.

[22] A. Van Pamel, G. Sha, S. Rokhlin, M. Lowe, Finite-element modelling of elastic wave propagation and scattering within heterogeneous media, Proc. Math. Phys. Eng. Sci. 473 (2197) (2017) 20160738, http://dx.doi.org/10.1098/rspa.2016.0738.

[23] A. Van Pamel, G. Sha, M. Lowe, S. Rokhlin, Numerical and analytic modelling of elastodynamic scattering within polycrystalline materials, J. Acoust. Soc. Am. 143 (4) (2018) 2394–2408, http://dx.doi.org/10.1121/1.5031008.

[24] M. Ryzy, T. Grabec, P. Sedlák, I.A. Veres, Influence of grain morphology on ultrasonic wave attenuation in polycrystalline media with statistically equiaxed grains, J. Acoust. Soc. Am. 143 (1) (2018) 219–229, http://dx.doi.org/10.1121/1.5020785.

[25] G. Sha, M. Huang, M. Lowe, S. Rokhlin, Attenuation and velocity of elastic waves in polycrystals with generally anisotropic grains: Analytic and numerical modeling, J. Acoust. Soc. Am. 147 (4) (2020) 2442–2465, http://dx.doi.org/10.1121/10.0001087.

[26] M. Huang, G. Sha, P. Huthwaite, S. Rokhlin, M. Lowe, Maximizing the accuracy of finite element simulation of elastic wave propagation in polycrystals, J. Acoust. Soc. Am. 148 (4) (2020) 1890–1910, http://dx.doi.org/10.1121/10.0002102.

[27] A. Boström, A. Ruda, Ultrasonic attenuation in polycrystalline materials in 2D, J. Nondestruct. Eval. 38 (2) (2019) 1–6, http://dx.doi.org/10.1007/s10921-019-0590-9.

[28] A. Boström, Scattering by a smooth elastic obstacle, J. Acoust. Soc. Am. 67 (6) (1980) 1904–1913, http://dx.doi.org/10.1121/1.384455.

[29] P. Waterman, Matrix theory of elastic wave scattering, J. Acoust. Soc. Am. 60 (3) (1976) 567–580, http://dx.doi.org/10.1121/1.381130.

[30] M. Huang, M. Lowe, Private communication, 2021.

[31] L. Yang, O. Lobkis, S. Rokhlin, An integrated model for ultrasonic wave propagation and scattering in a polycrystalline medium with elongated hexagonal grains, Wave Motion 49 (5) (2012) 544–560, http://dx.doi.org/10.1016/j.wavemoti.2012.03.003.
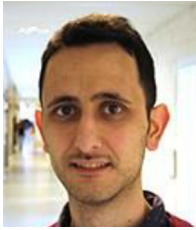
Ata Jafarzadeh obtained B.Sc. in Civil Engineering in 2015 from Ferdowsi University of Mashhad, Iran, and M.Sc. in Earthquake Engineering in 2018 from the University of Tehran, Iran. He started a Ph.D. in Mechanic in 2019 at Chalmers University of Technology, Gothenburg, Sweden. The main purpose of his Ph.D. project is to extend the possible type of analytical solutions by solving the canonical problem of elastic waves scattering by an anisotropic sphere.

Peter Folkow obtained a Ph.D. in Mechanics in 1998 at Chalmers University of Technology, Gothenburg, Sweden, and is now an associate professor at Chalmers. Since 2015 he is head of Division of Dynamics. He has published more than 25 papers in international journals. His research interests include wave propagation and vibrational problems in elastic media, primarily comprising analytical methods in structural elements. He has recently studied more applied fields, such as vibrational modeling for energy harvesters as well as blast vibrational problems in structures.

Anders Boström obtained M.Sc. in Engineering Physics in 1975 and Ph.D. in Mathematical Physics in 1980, both from Chalmers University of Technology, Gothenburg, Sweden. He became professor and chair in mechanics in 1986 at Chalmers and professor emeritus in 2018. Among other positions he has been head of department. He has supervised more than 20 Ph.D. students and has published more than 80 papers in international journals. His research interests include wave propagation and scattering in elastic solids, primarily with analytical methods, with applications in such areas as nondestructive evaluation, material characterization, and ground vibrations.